Clays and Clay Minerals, Vol. 43, No. 1, 14–28, 1995.

PARTICLE MORPHOLOGICAL EVOLUTION DURING THE CONVERSION OF I/S TO ILLITE IN LOWER CRETACEOUS SHALES FROM SERGIPE-ALAGOAS BASIN, BRAZIL

ANGÉLICA VARAJÃO[1,2] AND ALAIN MEUNIER[2]

[1] DEGEO Escola de Minas, UFOP, Campus Morro do Cruzeiro
35400 Ouro Preto MG, Brazil

[2] L.P.A.H, UA 721 C.N.R.S. University of Poitiers
40 Avenue du Recteur Pineau 86022 POITIERS Cedex, France

Abstract—The illitic end of mixed-layer illite-smectite series (I/S) in shales from Lower Cretaceous Barra de Itiúba Formation, Sergipe-Alagoas basin, was examined with X-ray powder diffraction (XRD) and transmission electron microscopy (TEM). A mathematical decomposition of XRD patterns shows different I/S and illite populations. All the samples contain ordered (R = 1) I/S, poorly crystallized illite (PCI) and well crystallized illite (WCI). A randomly interstratified (R = 0) I/S was also identified in a fractured zone at 1020 m. The percentage of expandable layers in ordered I/S decrease progressively from 20% to 10%. TEM observations show a continuous change in morphology between two basic particle shapes: elongated (lath) and isometric. The size and morphology of particles change with increasing depth. The proportion of laths decreases while isometric particles become predominant. However, both particle types continuously grow and enrich the larger size fraction. The growth process is driven by a mass transfer from the dissolving small particles of predominantly I/S (R = 1) composition to the larger (more illitic) lath and isometric ones. The proportion of lath-shaped particles decreases with depth indicating that the more stable population upon increased burial is the isometric well crystallized illite (WCI) particles. Very large laths are observed in the fault zone where conditions may favor faster growth processes.

Key Words—Illite, Illite/smectite, Morphology, Shale, TEM, XRD.

INTRODUCTION

The transformation of smectite-to-illite through a series of interstratified illite/smectite (I/S) clays is a common mineralogical reaction documented from various geological environments. It was extensively studied in burial diagenesis profiles of clastic sediments, especially from the Gulf Coast of the United States, in terms of compositional series of I/S where smectite layer percent (%Sm) decreases from smectite-rich rocks near the surface to illitic shales or sandstones a few kilometers at burial (Burst 1969, Perry and Hower 1970, Hower *et al* 1976, Boles and Franks 1979, Freed and Peacor 1989). Similar studies were also reported in other geological settings, including geothermal areas (Inoue *et al* 1987, 1988), contact metamorphism (Nadeau and Reynolds 1981), and thrust sheet burial (Hoffman and Hower 1979).

Scanning electron microscopy (Pollastro 1985, Inoue 1986, Keller *et al* 1986) and transmission electron microscopy (TEM) investigations (Inoue *et al* 1987, 1988) reveal dramatic changes of I/S crystal morphology. Three different shapes have been identified: sheets or flakes, laths, and hexagons which are attributed to randomly interstratified smectite-rich (R = 0) I/S, ordered (R = 1) I/S and highly illitic ordered (R ≥ 3) I/S or illite, respectively. Quantitative morphological data obtained from image processing of electron micrographs show that the sizes of both lath-shaped and isometric particles increase with increasing temperature-time conditions, and that isometric particles become the dominant population (Inoue *et al* 1988, Champion 1989, Lanson and Champion 1991). Ostwald ripening is the proposed process which controls grain-coarsening and layer thickening of the particles (Eberl and Środoń 1988, Inoue *et al* 1988, Eberl *et al* 1990). Quantitative studies of particle size and shape were only made for high porosity rocks (mainly tuffs and sandstones) of hydrothermal (Inoue *et al* 1987, 1988) and diagenetic environments (Champion 1989, Lanson and Champion 1991), where the growth process is unconstrained by pore size, and I/S and illite particles can exhibit free-growing crystal faces. The Ostwald ripening process implies two conditions: 1) the chemical system must be strictly closed, i.e., a constant mass of reactive internal chemical components; 2) the particles must have the same crystallochemical characteristics over the course of ripening process. Therefore, the distribution of particle size in the reduced coordinates remains constant whatever the temperature conditions. These two conditions of Ostwald ripening are not demonstrated for the diagenetic transformations of I/S (Lanson and Champion 1991); however, the size of the particles is distributed according to a log-normal law, which is similar to that of Ostwald ripening controlled by the second order reaction (Eberl *et al* 1990). If this is an Ostwald ripening process, the

elements feeding the growth of the largest particles are supplied by the dissolution of the smallest ones. The chemical exchange is complex in diagenetic reactions in which dissolving and growing crystals constitute multiphase assemblages. Thus little is known about the chemical balance of I/S "ripening".

The purpose of the present study is to investigate through quantitative analysis of size and shape, the growth mechanism of I/S (R = 1) particles in low porosity rocks subjected to progressive burial diagenetic conditions. Shale samples were selected from the Lower Cretaceous Barra de Itiúba formation in the Sergipe-Alagoas basin (Brazil). X-ray powder diffraction (XRD) was used to characterize the mineralogical evolution along the series and morphological characteristics were determined by TEM observations.

LOCATION AND GEOLOGICAL SETTING

The Sergipe-Alagoas basin is located on the Northeastern coast of Brazil (Figure 1). The sedimentation process in the basin has varied in time and space due to tectonics induced by the formation of the South Atlantic Ocean (Ponte and Asmus 1976). The basin is filled with up to 10 km of pre-rift, rift, and passive margin (post-rift) strata. Upper Paleozoic and Jurassic comprise pre-rift cratonic sequences. Thick sequences of Lower Cretaceous rift strata and superposed Upper Cretaceous/Tertiary passive-margin deposits complete the stratigraphic fill of Sergipe-Alagoas basin. The main tectonic framework of the Sergipe-Alagoas basin is characterized by half-graben structures which have formed lower regions and several platforms located Southeast of the basement-bounding fault. The initial faulting occurred during the early Cretaceous rift phase; it is responsible for most of the present structural features in the basin (Fernandes *et al* 1981).

The study area includes two fault-bounded blocks: the São Miguel dos Campos Platform (wells: Fu-1, CSMC and SMC) and the lower Barra de São Miguel region (BSM well; Figure 1). The stratigraphic sequence is incomplete in both areas. Erosion surfaces account for the absence of post-Lower-Cretaceous sediments. In the lower Barra de São Miguel region, the sequence is slightly thicker. This study concentrates on the shales of the Barra de Itiúba Formation, which represents an initial rift deposition stage of deltaic-lacustrine system, which is composed of over 2000 m of sediments in the lower region (Figure 1).

EXPERIMENTAL

Sampling

One hundred twenty three (123) samples from drill cuttings and cores in four wells at depths ranging from 550 m to 3500 m were collected at intervals ranging from 40 m to 90 m. Shale chips were hand-picked from cuttings under a binocular microscope and gently

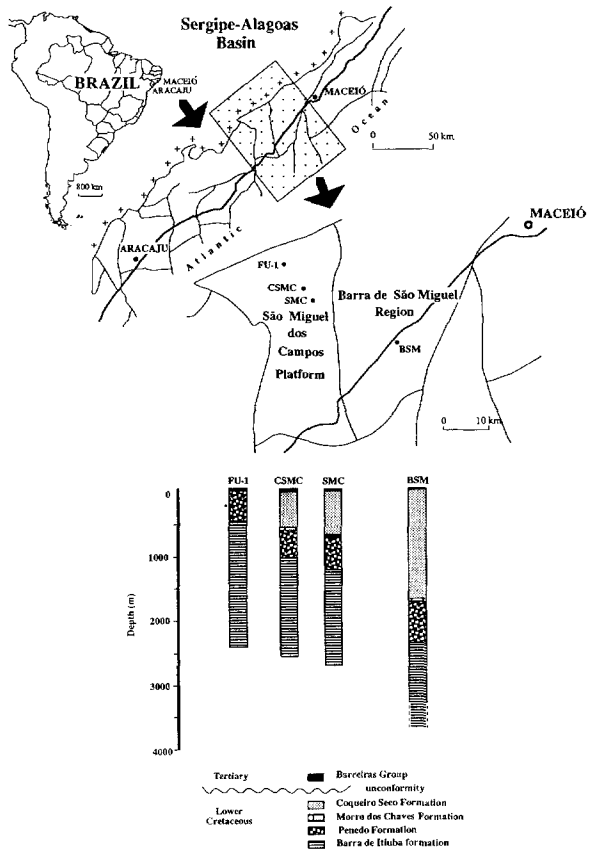

Figure 1. Location map and simplified stratigraphic sequence of the studied wells (Fu-1, CSMC, SMC and BSM).

washed with distilled water to remove any remaining drilling mud. Seventy two (72) samples representing the general diagenetic evolution in the studied series were selected for detailed XRD analysis of the $<2\ \mu m$ fraction. Finally, five samples: 615 m, 1020 m, 1827 m from Fu-1 well and 2871 m, 3325 m from BSM well were chosen for morphological studies. The 1020 m sample is from a fractured zone that represents a structural discontinuity (probably in the vicinity of a fault); the four remaining samples represent undisturbed diagenetic sequence and the complete range of the I/S crystalline state in the drilled series.

X-ray powder diffraction and decomposition method

All samples were crushed in an agate mortar and ultrasonically dispersed in distilled water. The $<2\ \mu m$ fraction was separated from suspension using standard sedimentation procedures. A routine mineralogical identification by XRD (Philips PW 1730 diffractometer, CoKα radiation, 40 kV, 40 mA, Fe filter) of all samples was performed on randomly-oriented whole-rock and on oriented specimens of the $<2\ \mu m$ fraction after air drying (AD) and ethylene-glycol vapor saturation (EG) for at least 48 hours.

https://doi.org/10.1346/CCMN.1995.0430103 Published online by Cambridge University Press

The <2 μm fraction of seventy two samples were analyzed once again after AD and EG using a Philips PW 1729 diffractometer (CoKα radiation, 40 kV, 40 mA, Fe filter) equipped with a stepping motor (SOCABIM DACO system). Numerical XRD patterns were recorded in 2°–35 °2θ angular range using 0.025 °2θ step and 6 s/step counting time.

XRD patterns (AD) were decomposed into Gaussian and Lorentzian elementary bands using the DECOMPXR program of Lanson (1990). Details of this method have been described by Lanson and Besson (1992) and Lanson and Velde (1992). We shall use the terminology defined by these authors in which the term crystallinity is taken as an equivalent of coherent scattering domain size (CSDS): I/S for ordered illite-smectite mixed-layered minerals (%Sm > 5%), PCI for poorly crystallized illite or illite-rich mixed-layered minerals (%Sm < 5%), and WCI for well crystallized illite. I/S and PCI are characterized by a small (CSDS) and WCI is characterized by a large CSDS. For all decompositions the best fit was achieved assuming Kα_1 and Kα_2 contributions to be both Gaussian for I/S populations and both Lorentzian for chlorite. For illite (WCI, well crystallized illite) the shapes of Kα_1 and Kα_2 are assumed to be Gaussian and Lorentzian, respectively.

According to Lanson and Besson (1992), long-range stacking junction probabilities (R ≥ 2) have no physical meaning even for highly illitic material. They consider that the occurrence of a given layer will depend only on its nearest neighbors and not on greater distance neighbors. A detailed discussion is given in Lanson and Besson's paper. For this reason, we have considered the I/S ordering type as R = 1 whatever the smectite content. The smectite content of I/S was determined on air-dried oriented preparations according to the following procedure:

1) The position of the I/S peak was measured on natural samples. Hydration state is critical to determine I/S composition using air-dried samples (Sato *et al* 1992). To assure a two-layer hydration at typical laboratory humidity, saturations with a single cation were used in the separation procedures of some samples (Jackson 1974). Due to the variable hydration state presented by Na^+, saturations with Ca^{2+} were preferred when using the air-dried determinative method (Velde *et al* 1986). The results show that the position of the I/S peak is similar in the natural and Ca-saturated states and is coherent with a two water layer model for the smectite component;
2) The measured positions were plotted in a %Sm versus position diagram obtained from calculated XRD patterns using the NEWMOD software (Reynolds 1985): coherent scattering domains (N): from 4 to 10; smectite hydration state: two water layers; Fe: 0.3; K: 0.8.

The relative proportions of chlorite, I/S, PCI and WCI were estimated from the intensity of their peaks in the decomposed range (5–12.5 °2θ CoKα): WCI% = WCI intensity × 100/Σ intensities (Chlorite + I/S + PCI + WCI). These estimations have no global quantitative meaning but they can be used to compare the five samples selected for the morphological study.

TEM and image analysis

Clay particle morphology was studied using the method described by Inoue *et al* (1987), Inoue *et al* (1988), Champion (1989) and Lanson and Champion (1991). A highly diluted suspension of the <2 μm fraction was prepared in distilled water and clay particles were dispersed by ultrasonic treatment. A drop of the suspension was deposited on a carbon-coated copper grid and dried at room temperature. Observations were made using a JEOL 100S & SX (Philips 100Kv) TEM; 6 to 10 micrographs were taken for each sample in order to define the contours of 400–600 grains. The grain shapes were copied on tracing paper, filled with black and subsequently scanned (Image-in, public domain software).

Area and shape were determined using the ANAFORM program (Touchard *et al* 1993). A circumscribed rectangle is drawn around each particle. Additionally, every particle is represented by an "equivalent" rectangle whose edges are the particle mean length and width. Four parameters were thus obtained for each particle: length (L), width (W) and mean length (Lm), mean width (Wm) from the circumscribed rectangle and the equivalent rectangle, respectively. These parameters were used to estimate a shape ratio (S_R = L/W) and the area (S = Lm × Wm). The equivalent diameter ($D = 2(S/\pi)^{0.5}$; Champion 1989) for each particle was quantified considering that the mean dimensions of the rectangle are identical to the axes of the ellipse inscribed on each grain convex outline. This equivalent diameter was used to obtain the normalized diameter distribution.

RESULTS

XRD analyses show that the mineralogical composition of the <2 μm fraction is similar to that of the bulk rock. The 123 investigated samples contain quartz, calcite, K-feldspar, plagioclase, chlorite, I/S (R = 1) mixed layered minerals and illite (or mica). Analcime and kaolinite are present only in the three wells from the São Miguel Platform. Kaolinite occurs in the upper part and analcime in the lower of these wells. The noncoexistence of kaolinite and analcime is explained by changes in the sedimentary environment. Kaolinite belongs probably to the detrital mineral set while analcime was formed during early diagenetic processes. Indeed, subaerial exposure of sediments in deltaic-lacustrine systems induces the concentration of sodium carbonates that react with clay minerals forming anal-

https://doi.org/10.1346/CCMN.1995.0430103 Published online by Cambridge University Press

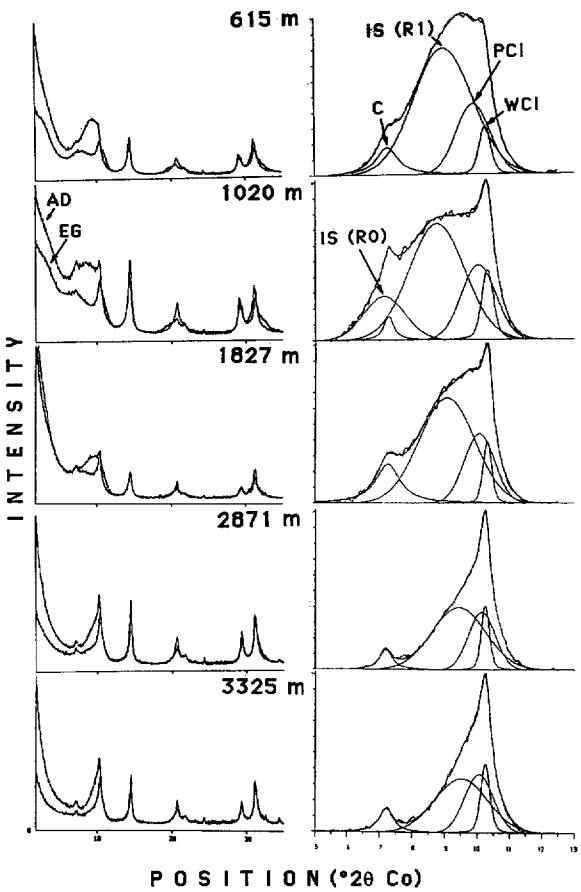

Figure 2. X-ray powder diffraction profiles (CoKα radiation) of oriented <2 μm fraction specimens after air-dried (AD) and ethylene-glycol (EG) saturation (left) and decomposition of AD profiles in the 5–12.5 °2θ CoKα range (right). C = chlorite; IS (R0) = randomly interstratified I/S; IS (R1) = ordered I/S; PCI = poorly crystallized illite; WCI = well crystallized illite.

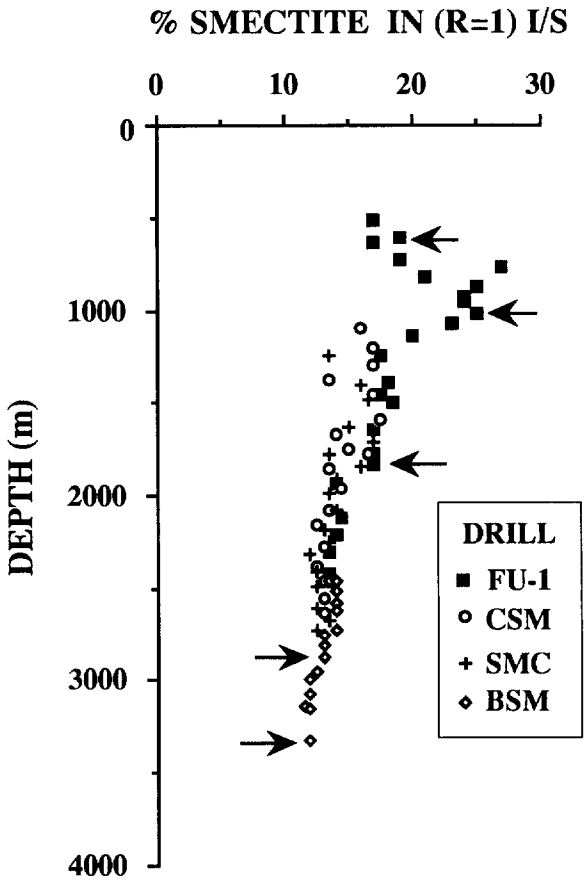

Figure 3. Percent smectite-layers content in I/S (R = 1) versus depth for the four wells studied. Arrows indicate the samples selected for the morphological study.

cime (Hay and Moiola 1963, Hay 1970, Remy and Ferrel 1989).

Clay minerals were studied in detail in the <2μm fraction of 72 samples. For most of them four elementary curves were used to obtain an acceptable fit in the low angle range (5–12.5 °2θ CoKα). According to the peak position and the full width at half maximum intensity (FWHM), each curve is attributed to the following mineral species (Figure 2): chlorite, (R = 1) I/S, a poorly crystallized illite (PCI) and a well crystallized illite (WCI). The decomposition procedure fails to distinguish the respective contribution of detrital mica and of well crystallized authigenic illite (Lanson and Velde 1992). This ambiguity will be solved by the study of particle morphologies through TEM observations. Particles of detrital micas cannot have regular crystalline shapes as authigenic ones do. Besides, detrital micas were shown to have been totally transformed in the deepest part of other diagenetic series where illite-rich ordered I/S crystallize (Hower *et al* 1976, Velde *et al* 1986). One can consider that the narrow 10 Å peak represents only the WCI phase. The peak position of the ordered (R = 1) I/S phase shifts from 8.8 to 9.7 °2θ CoKα indicating that the proportion of illite layers increases from 80% to 90% with depth (Figure 3).

Samples from the 750–1050 m depth range (fault zone) of the Fu-1 well show an opposite trend: the (R = 1) I/S peak position varies from 8.8 to 8.6 °2θ CoKα indicating that the %Sm varies from 20 to 30%. It was necessary to add a fifth curve to get a good fit. This elementary curve represents a randomly interstratified (R = 0) I/S (Figure 2, 1020 m depth). The structural discontinuity appears to locally modify the porosity and permeability conditions and consequently affects the illitization reaction.

One of the five samples chosen for the morphological study comes from this unconformity range; its estimated smectite percentage in (R = 1) I/S is about 25%. The other four samples are from the undisturbed interval at 615 m, 1827 m, 2871 m and 3325 m. Table

https://doi.org/10.1346/CCMN.1995.0430103 Published online by Cambridge University Press

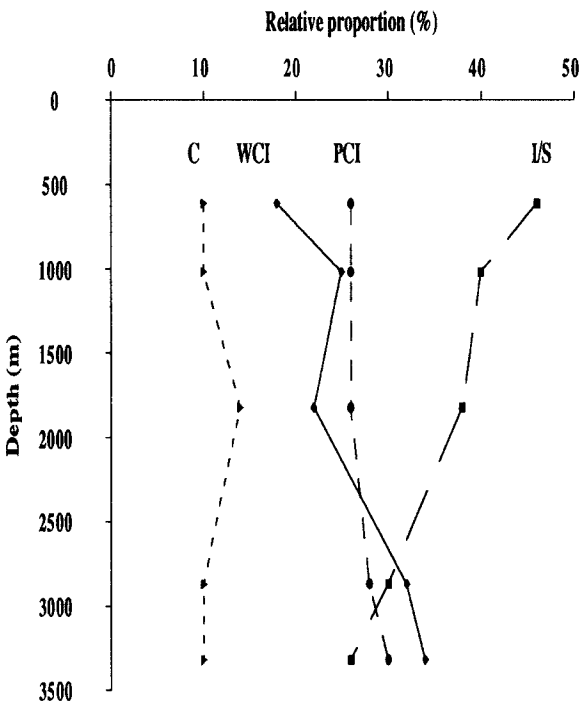

Figure 4. Semi-quantitative <2 μm clay mineralogy versus depth calculated from relative peak intensities after decomposition. C = chlorite; PCI = poorly crystallized illite; WCI = well crystallized illite; I/S = (R = 1) ordered I/S.

1 gives the spacing (Å) in air dried state of the three mineral species considered (I/S, PCI and WCI) for the five samples studied. The relative proportions of chlorite, (R = 1) I/S, PCI and WCI, for these five samples, is given in Figure 4. The typical morphology and size of particles are displayed in Figure 5. Considering that chlorite content is roughly equal and about 10%, the major grain morphologies are assumed to represent I/S and illite. Results of quantitative image analysis are presented in the form of frequency histograms for the surface area and shape ratio distributions.

The surface area histograms (Figure 6) are unimodal but asymmetrical towards upper values. The asymmetry is due to the presence of a few large particles. The histograms widen progressively with depth (the mean surface area increases from 0.00304 to 0.00536 μm^2), indicating that the number of large particles increases. The shape ratio (S_R = L/W) histograms are also unimodal and asymmetrical because of the presence of elongated lath-shaped particles (Figure 7). S_R shifts toward smaller values with increasing depth. One should note that S_R is equal to 1 and 1.14 for a perfect circle and a regular hexagon, respectively. This suggests a progressive transformation of lath-shaped particles into more isometric particles with increasing depth. The hexagonal particles commonly described in hydrothermally altered rocks (Inoue *et al* 1987, 1988) and in porous sandstones (Champion 1989, Lanson and Champion 1991) were not observed in the shales studied here. Instead, the isometric particles (isometric in the ab plane) frequently display two or three well defined growth faces.

Table 1. Spacing (Å) in air-dried state of I/S (R = 1), PCI and WCI at different depths.

Depth (m)	I/S (R = 1)	PCI	WCI
615	11.43	10.37	10.00
1020	11.71	10.23	9.96
1827	11.32	10.20	9.96
2871	10.89	10.13	10.02
3325	10.79	10.20	10.01

The asymmetry of the shape ratio (S_R) histograms is due to a progressive transition between lath-shaped and isometric particles. In order to calculate the change in the relative proportions of both particles an arbitrary value of S_R = 1.7 was taken as the limit between lath-shaped (S_R > 1.7) and isometric-shaped particles (S_R < 1.7) in the five samples. The proportion of isometric-shaped particles increases with depth from 46% to 70% at the expense of lath-shaped ones (Figure 7).

Surface area histograms can be established for isometric and lath-shaped particle populations. These histograms are asymmetrical (Figure 8). The mean surface area for isometric particles increases from 0.00278 to 0.00511 μm^2 and that for lath-shaped particles from 0.00328 to 0.00659 μm^2. The sample from 1020 m is anomalous if compared to the others: the surface area or the shape ratio (S_R) histograms (Figures 6 and 7) show that large particles are more abundant and mostly lath-shaped (Figure 8).

DISCUSSION

The <2 μm fraction of shales in the Barra de Itiúba formation is mainly composed of three dioctahedral populations: I/S of R = 1 type, PCI and WCI. WCI increases at the expense of I/S with depth. TEM observations show a continuous morphological change (unimodal histograms) between two types: elongated and isometric particles. The mean size of both particle types increases with depth and the relative proportion of isometric particles increases at the expense of lath-shaped ones. Moreover, the shape ratio (S_R) of the lath-shaped particles decreases with depth, indicating progressively isometric morphology. From these facts, it is apparent that the composition (%Sm), the size and the shape of clay particles change in the course of the diagenetic formation of illite layers.

The main difficulty in interpreting XRD data and morphological analyses of clay minerals is to define what are the relations between the observed particle populations and the concept of mineralogical phase. Indeed, considering the composition (%Sm), there are two phases: I/S and illite, but three particle populations

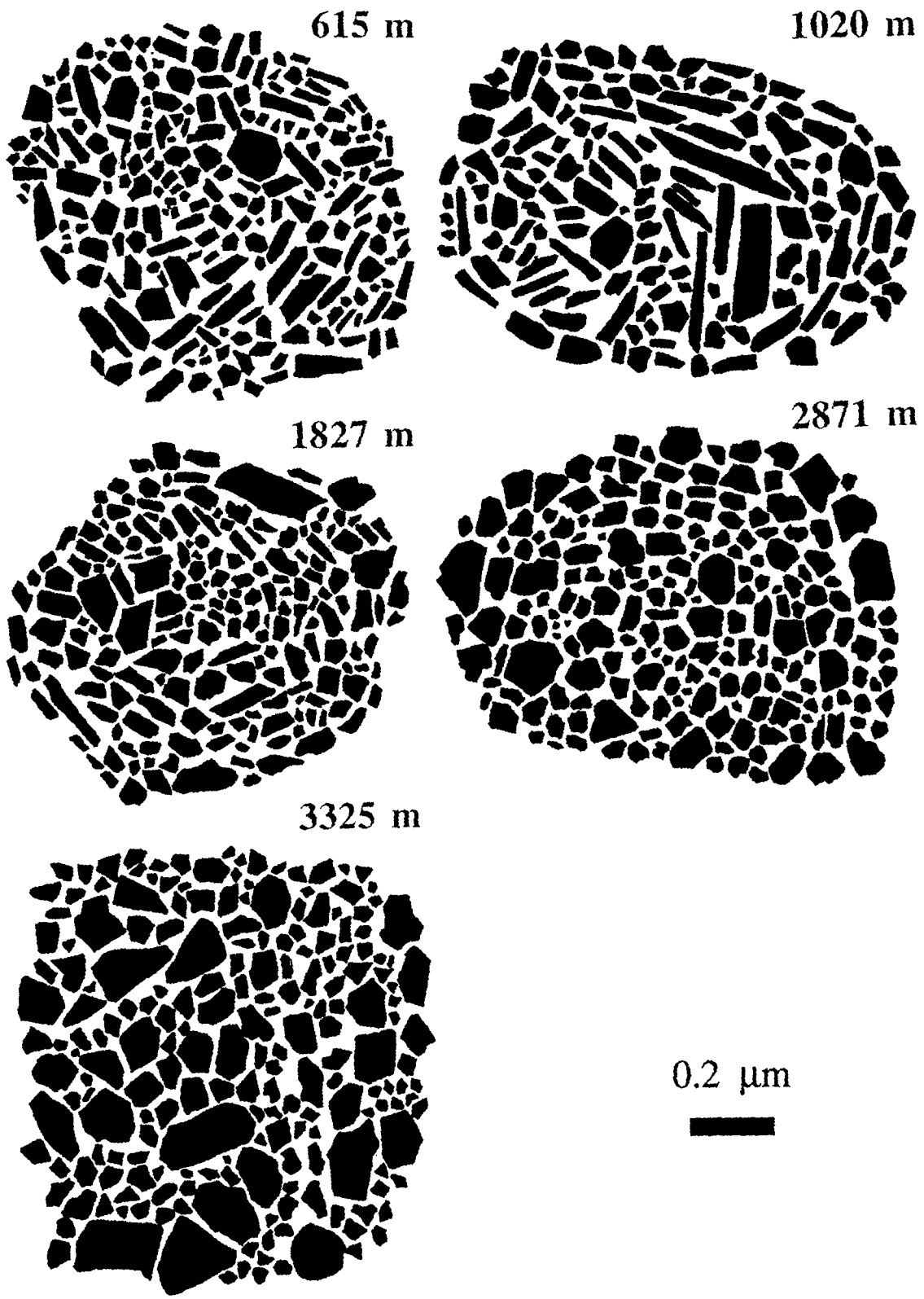

Figure 5. Morphology and size of the particles in the five samples studied from TEM micrographs (redrawn from TEM photographs). Note that the lath-shaped particles are clearly more abundant in the shallower samples than in the deeper ones in which large isometric particles are predominant.

https://doi.org/10.1346/CCMN.1995.0430103 Published online by Cambridge University Press

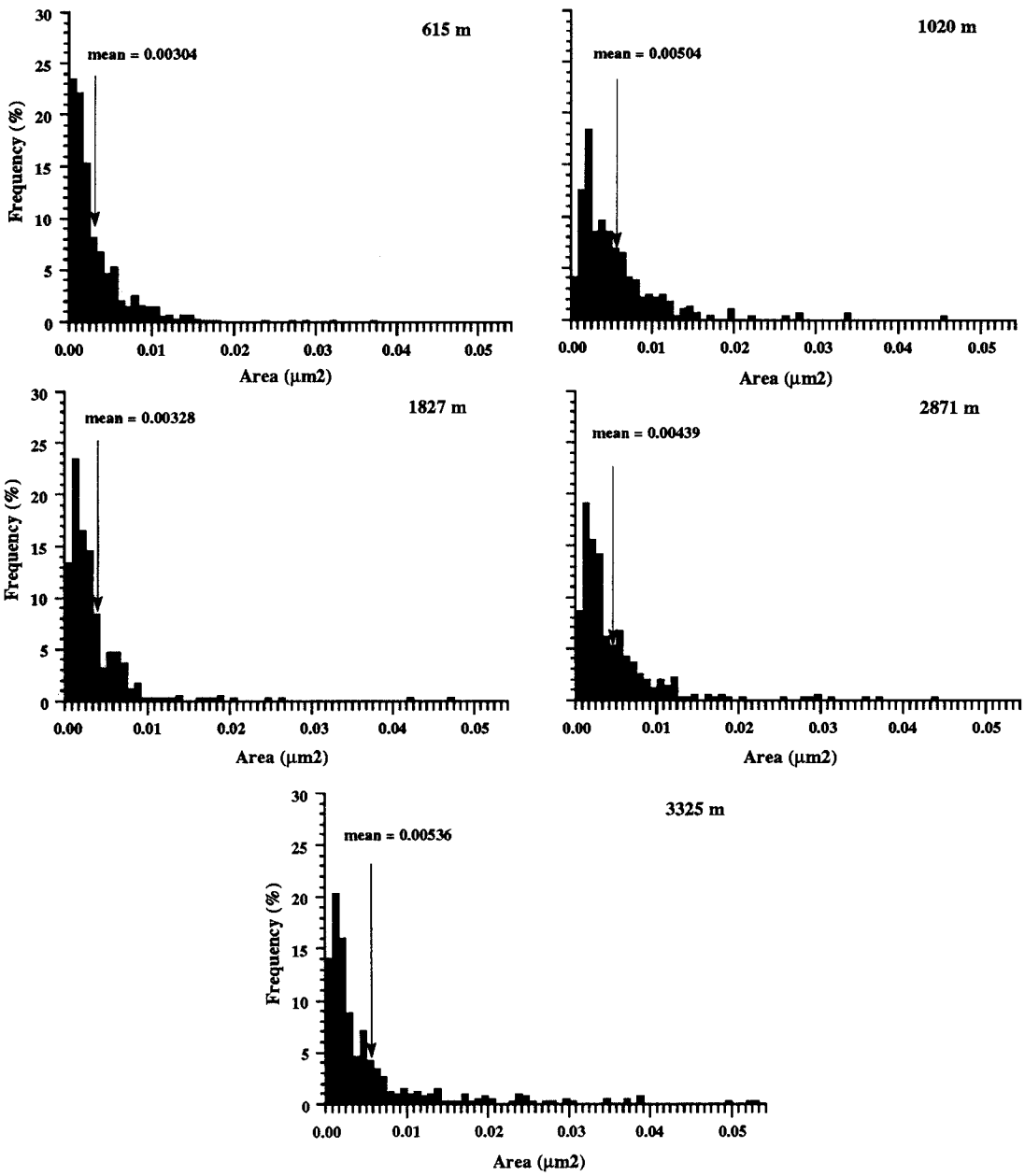

Figure 6. Histograms of particle surface areas. Note that histograms show an increasing asymmetry with depth indicating that the number of larger particles increases.

can be distinguished according to XRD profiles decomposition: I/S, PCI, and WCI. Morphologically, only one population is observed because the S_R ranges from 1 to 5, i.e., from isometric to elongated lath-shaped particles. In spite of this difficulty, the diagenetic evolution of composition (%Sm), ordering, size, and shape with increased burial conditions allow us to address the following questions: 1) which particles experience dissolution or growth with increasing diagenetic conditions? 2) what are the growth mechanisms for lath-shaped and isometric particles? 3) what might be the relations between I/S, PCI, and WCI determined by XRD, and size and shape of particles measured by TEM?

The undisturbed diagenetic sequence

Mass transfers. Theoretically, calculations of mass transfer from small to large particles, both in the lath-shaped and isometric particle populations must be based on the determination of mass (volume × density) of

https://doi.org/10.1346/CCMN.1995.0430103 Published online by Cambridge University Press

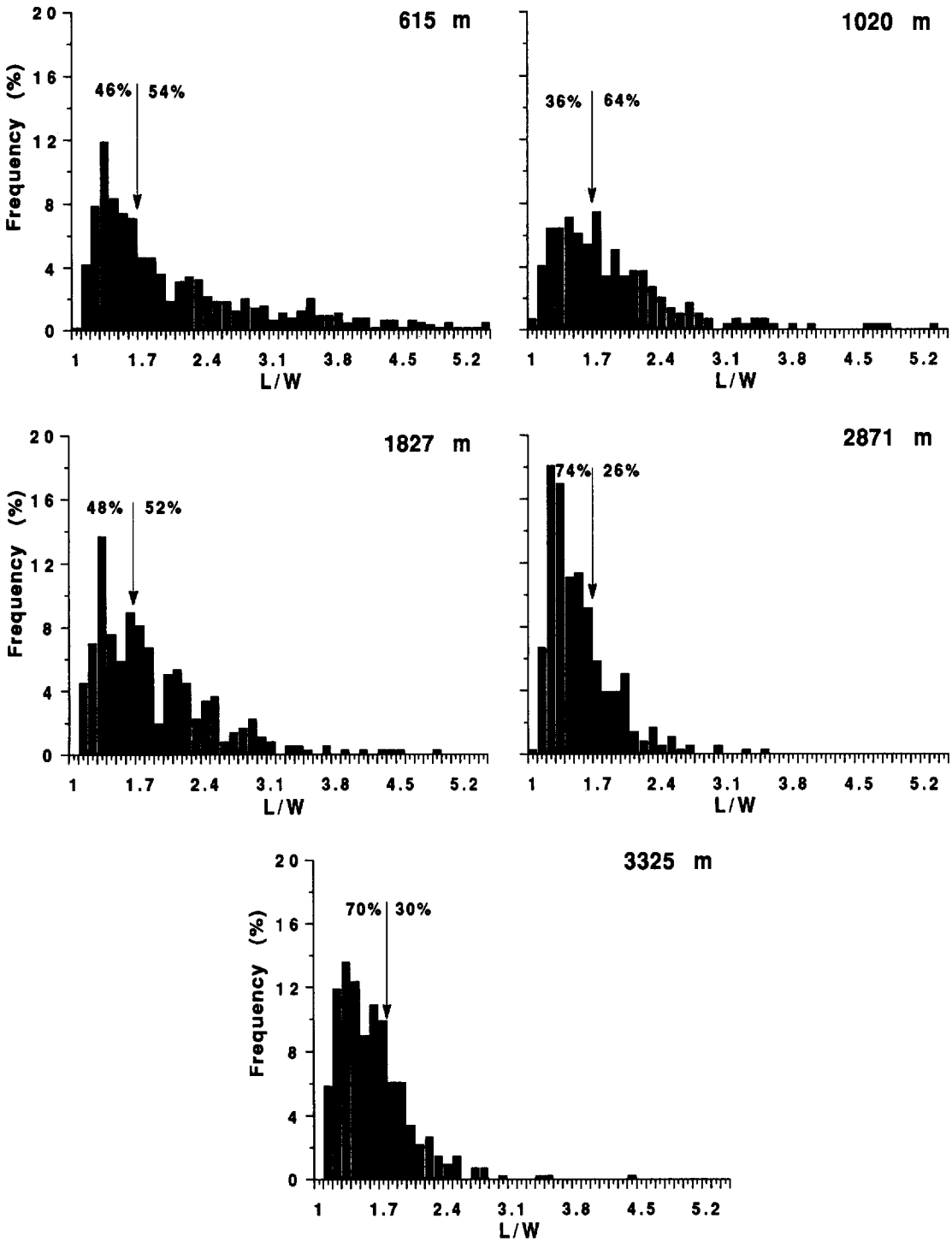

Figure 7. Histograms of shape ratio L/W (length/width). L/W ratio of 1.7 was taken as the limit between lath-shaped (S_R > 1.7) and isometric (S_R < 1.7) particle populations.

https://doi.org/10.1346/CCMN.1995.0430103 Published online by Cambridge University Press

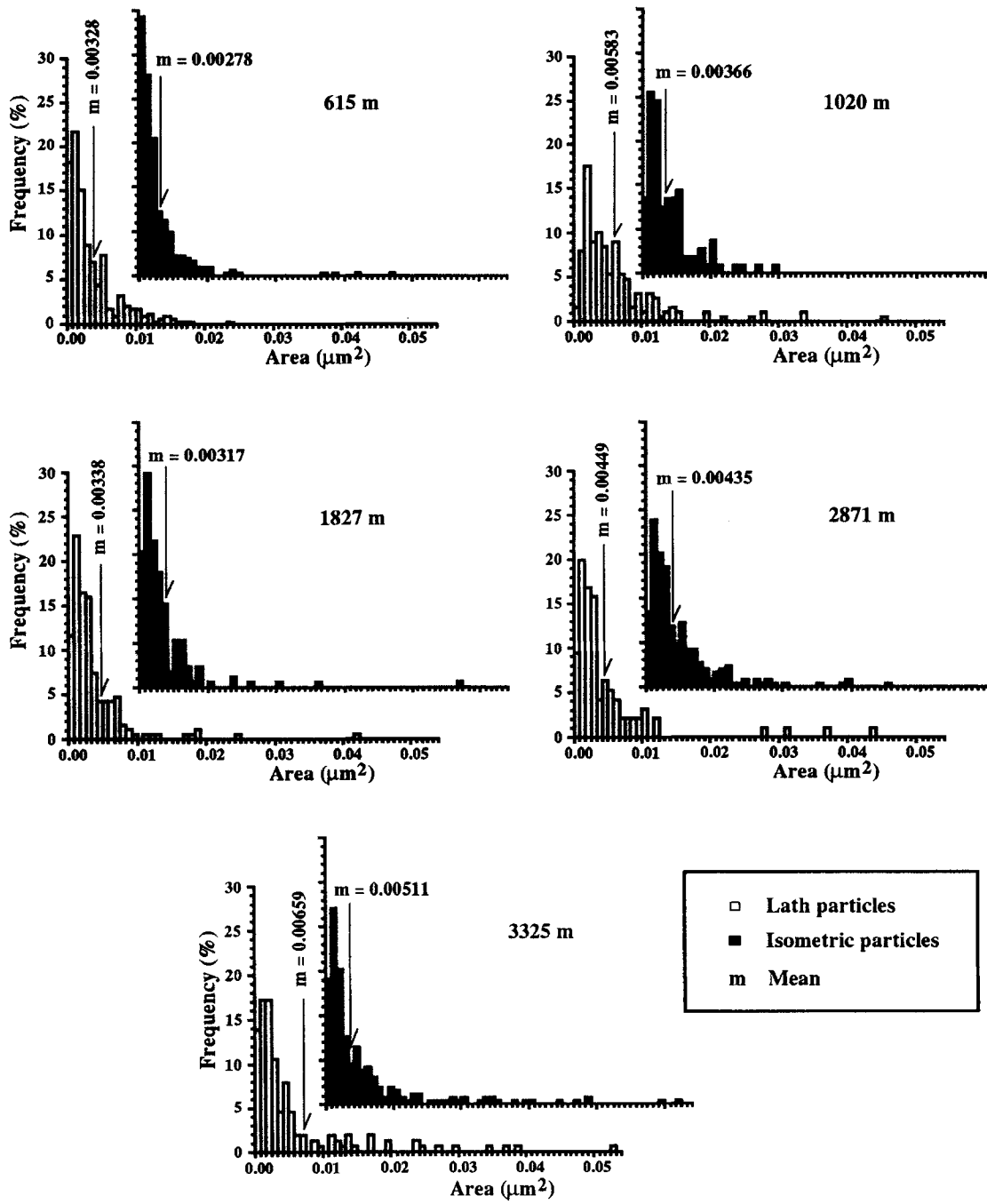

Figure 8. Histograms of surface areas for both lath-shaped and isometric particle populations. The mean area (m) of both lath and isometric particles increases with depth.

each category. Unfortunately, volume and density cannot be routinely measured on individual particles, thus direct mass calculations are not possible. Nevertheless, mass transfers between lath-shaped and isometric particle populations can be estimated semi-quantitatively comparing their relative quantities obtained multiplying the measured surface area by the frequency. According to the empirical relation of Nadeau (1985), area and volume are proportional, which validates our procedure. The product of frequency × surface area can then be considered representative of the mass of particles. Results are presented in the form of frequency × surface area versus surface area histograms in Figure 9. The <2 μm fraction is representative of the whole

https://doi.org/10.1346/CCMN.1995.0430103 Published online by Cambridge University Press

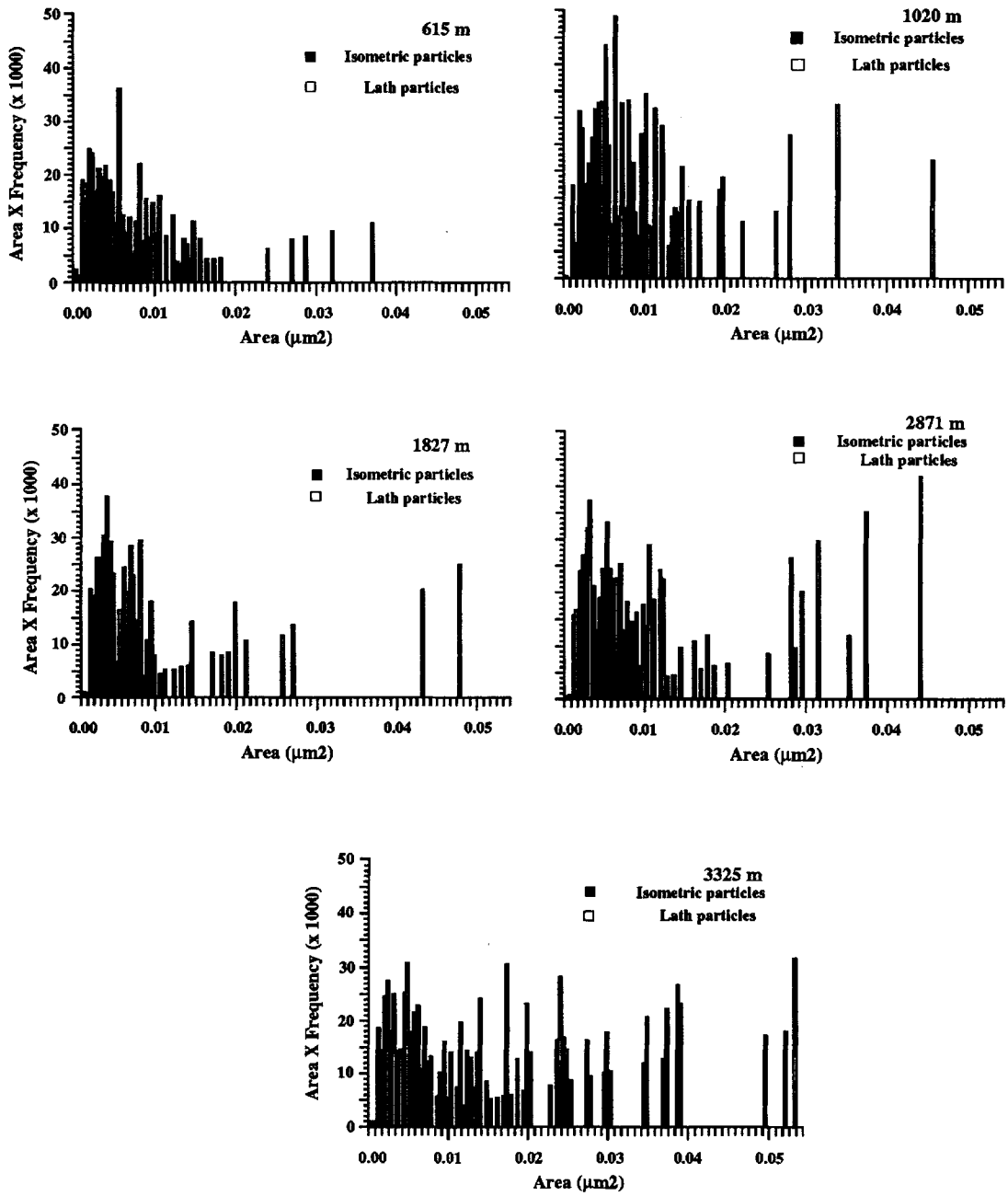

Figure 9. Histograms showing the repartition of mass (estimated as area × frequency) as a function of surface area for both lath-shaped and isometric particle populations. The mass of both lath-shaped and isometric particles of surface area > 0.016 μm^2 increases with depth (spread of the histograms).

mass of the clays because particles are rarely larger in the studied shales. The major part of the <2 μm fraction mass (lath-shaped as well as isometric particles) of 615 m sample is concentrated in particles whose surface area is lower than 0.016 μm^2. Then, mass transfer will be calculated considering the 615 m as a "starting point". A transfer parameter (Tr) is determined for each sample:

$$Tr = \Sigma\ (>0.016\ \mu m^2\ \text{particles})/\Sigma\ (\text{all particles})$$

Figure 10 shows that Tr increases linearly from 615 m to 2871 m; below this depth Tr increases sharply. It must be noted that the 1020 m sample is on the correlation line. The evolution of I/S with depth in diagenetic environments was shown to be a kinetic controlled phenomenon (Velde and Vasseur 1992). In

https://doi.org/10.1346/CCMN.1995.0430103 Published online by Cambridge University Press

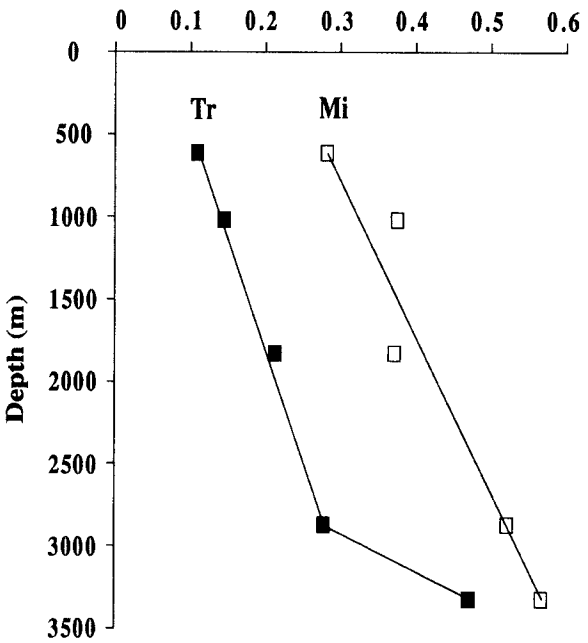

Figure 10. Variation of Tr parameter (Tr = Σ (>0.016 μm^2 particles)/Σ (all particles)) ratio and Mi parameter (Mi = WCI%/(WCI% + I/S%) with depth.

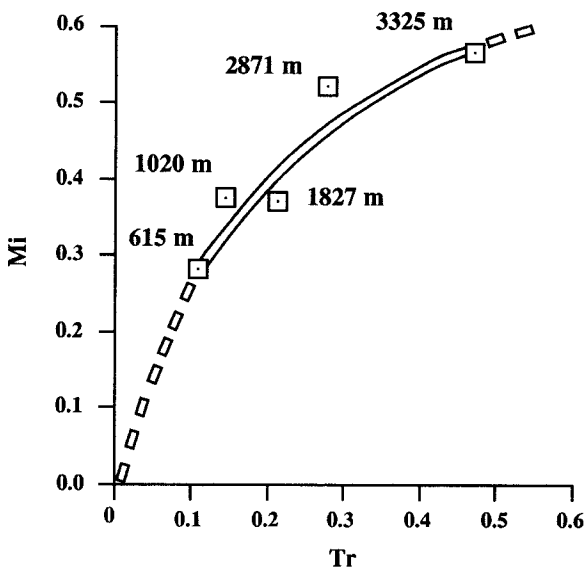

Figure 11. Mi parameter plotted against the mass transfer (Tr parameter). Tr = Σ (>0.016 μm^2 particles)/Σ (all particles); Mi = WCI%/(WCI% + I/S%).

other words, depth is the equivalent of a temperature-time parameter. The relationship observed in Figure 10 suggests that mass transfers from small to large particles are dependent of increased time-temperature conditions due to burial depth in the upper part of the diagenetic series. These transfers are strongly activated in the deepest part of the diagenetic series.

Relative proportions of both chlorite and PCI do not change significatively with depth (Figure 4). From the mineral data, diagenetic reactions induce a progressive increase of WCI at the expense of I/S. Thus the reaction progress can be expressed by the following mineralogical parameter (Mi):

$$Mi = WCI\%/(WCI\% + I/S\%)$$

The Mi parameter increases progressively with depth from 615 m to 3500 m (Figure 10). The increase of WCI% can be explained in two ways: 1) the increase on the number of WCI particles; 2) the thickening of the coherent scattering domain size (CSDS) of WCI. As shale diagenesis is considered an isochemical process with respect to the whole rock chemistry (except for water), if the size of particles increases their number must decrease. If so, the increase in Mi with depth suggests a progressive thickening of WCI particles, perhaps due to the formation of additional illite layers (growth process).

How does mass transfer lead to the thickening of existing WCI particles? Figure 11 shows that the Mi-Tr relationship is not linear. This suggests that the increase of WCI% is not simply proportional to the mass transfer from dissolving small particles to growing large ones. Indeed, WCI% increases sharply from 0 to 2871 m and then slowly from 2871 m to 3325 m. This could be due to the fact that the addition of a new illite layer on a particle (thickening) needs more and more matter as the size increases.

Stable and metastable shapes of particles. The presented data show that both lath-shaped and isometric particles with a surface area > 0.016 μm^2 grow simultaneously. Nevertheless, isometric particles predominate with increasing diagenetic conditions; i.e., increased burial (Figure 12a). Such relationship has been described by Lanson and Champion (1991) in sedimentary sequence from the Paris basin. However, little is known about the relative rate of growth. Figure 12b shows that lath-shaped particles grow faster than isometric ones in the 615 m to 2871 m part of the diagenetic series. For larger depths, this trend is reversed and the isometric particles become predominant; which means that large lath-shaped particles are dissolved in the deepest part of the series. These particles could be considered as a metastable state of WCI particles, the stable state being the isometric ones (equivalent of hexagons described in porous sandstones by Lanson and Champion 1991).

The remaining question is: which particles belong to the PCI category? Although the data indicate that the relative PCI intensity on XRD patterns is relatively constant, these particles are probably not chemically inert. This means that the bulk diffracting properties (quantities and CSDS of particles) remain roughly constant, which is possibly due to a balance between dis-

https://doi.org/10.1346/CCMN.1995.0430103 Published online by Cambridge University Press

solving and growing particles. Therefore, the PCI population is necessarily composed of different kinds of particles: lath-shaped particles in which illite layers have grown on an I/S nucleus, and small isometric particles which composition is purely illitic. A similar process was revealed by Pollastro (1985), who has shown from textural observations and relationships from SEM studies, an aggrading of PCI with increasing smectite-illite reaction. The PCI particles are characterized by a low CSDS (Lanson and Besson 1992).

The fault zone (−1020 m)

The <2 μm fraction of the 1020 m sample is predominantly composed of large lath-shaped particles. Lath-shaped particles with surface area larger than 0.016 μm^2 represent about 14% of the total mass (Figure 9). In spite of this difference from the samples representing the undisturbed diagenetic sequence, the values of the Tr and Mi parameters of the 1020 m sample are coherent with the general trend indicated in Figure 10. This means that the quantity of dissolved small particles is dependent on burial depth, i.e., time-temperature conditions at a given depth, as in all the diagenetic series. On the other hand, the precipitation of illite layers in the fault zone is accelerated, producing large lath-shaped particles. The period of time during which the fault zone was opened to fluid circulation was much shorter than burial diagenesis reaction. Mass transfer was possibly accelerated by the presence of higher quantities of fluids, because permeability was increased in the fault zone. This could be compared to hydrothermal alteration of shales, which first produces large lath-shaped illite before platy illite (Glassmann *et al* 1989). The predominance of large lath-shaped particles and the relatively high WCI% in the 1020 m sample, compared to the following one in the undisturbed series (−1827 m), suggests that these particles are purely illitic. In other words, the fastest way of WCI crystallization leads to the formation of lath-shaped particles. These particles must be considered as a metastable state of WCI since the stable one is the isometric or hexagonal shape.

Growth mechanisms

The growth mechanism can be estimated indirectly from the grain-size distribution. Baronnet (1982) has reviewed the theoretical aspects of this analysis which uses reduced coordinate histograms. Inoue *et al* (1988), Eberl and Środoń (1988), and Eberl *et al* (1990) showed that the particle-size distribution during the smectite-to-illite conversion is controlled by the Ostwald ripening process. Eberl *et al* (1990) characterized this steady-state profile by a log-normal distribution curve whose equation is:

$$f(\omega) = \frac{1}{\omega\beta\sqrt{2\pi}} \exp\left\{-\left(\frac{1}{2\beta^2}\right)[\ln(\omega) - \alpha]^2\right\}$$

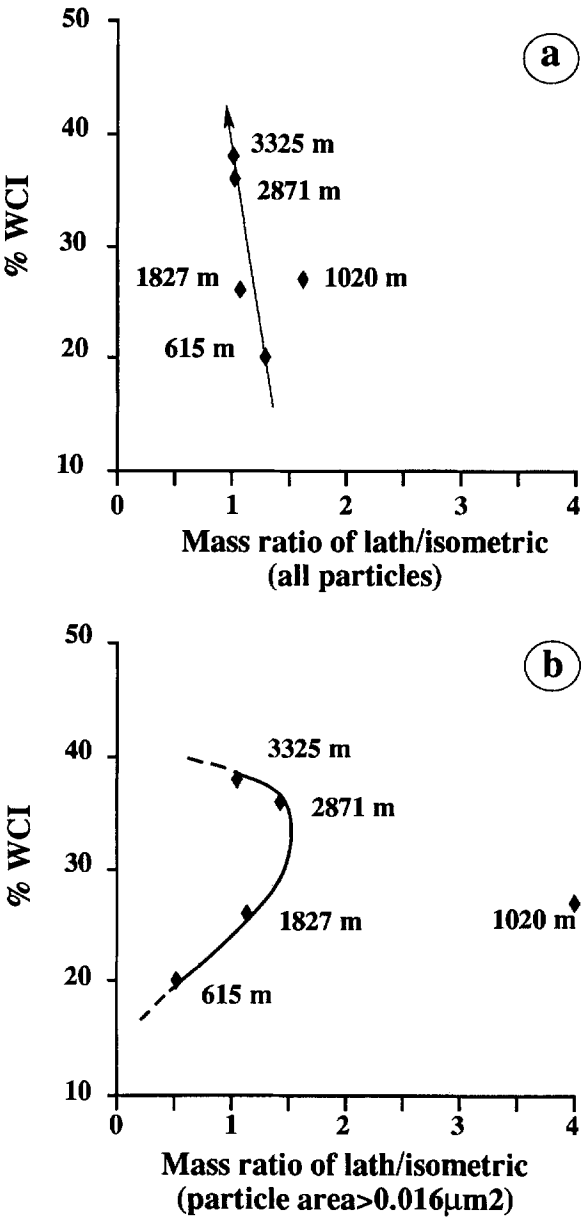

Figure 12. Relation between percentage of well crystallized illite (WCI%) in the clay fraction and the mass of lath-shaped and isometric particles. a) All the particles are considered; b) only large particles (area > 0.016 μm^2) are considered.

where:

$-f(w)$ = the frequency of the observations w.

$-\beta^2 = \Sigma\,[\ln(\omega) - \alpha] f(\omega^2)$

= the variance of logarithms of the observations

$-\alpha = \Sigma\,[\ln(\omega) f(\omega)]$

= the mean of the logarithms of the observations

https://doi.org/10.1346/CCMN.1995.0430103 Published online by Cambridge University Press

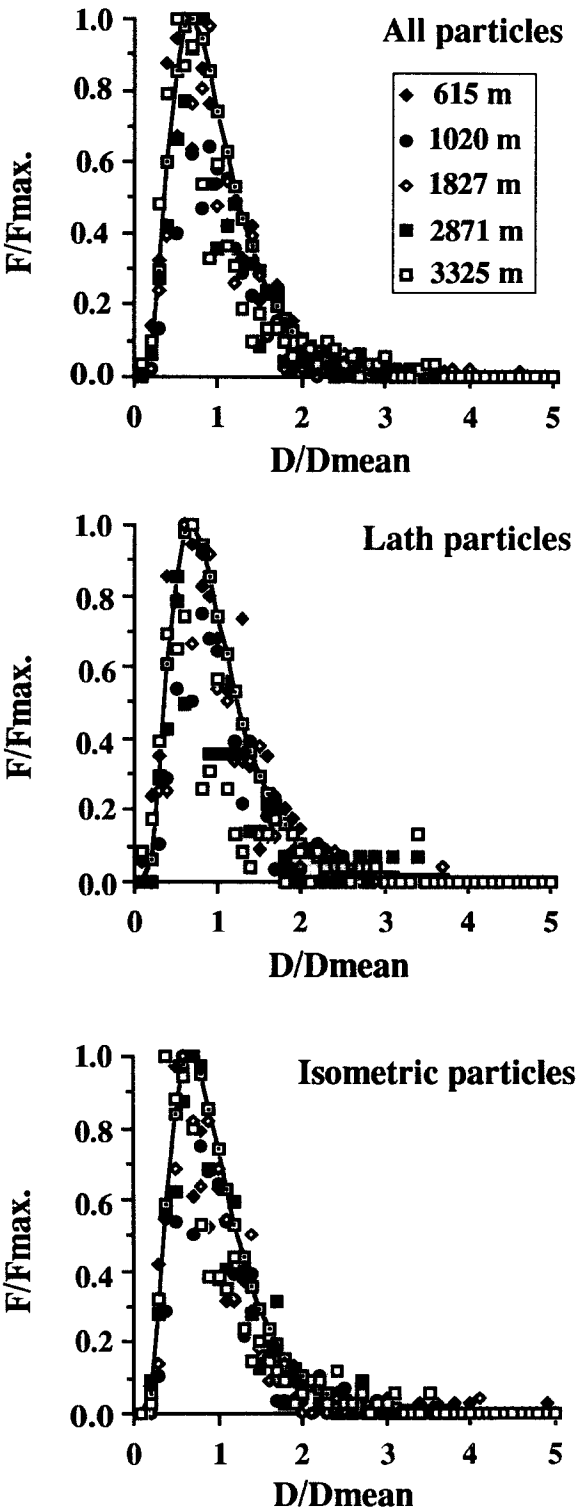

Figure 13. Equivalent diameter of particles represented on reduced coordinates. The log-normal distribution was calculated by the equation proposed by Eberl *et al* (1990).

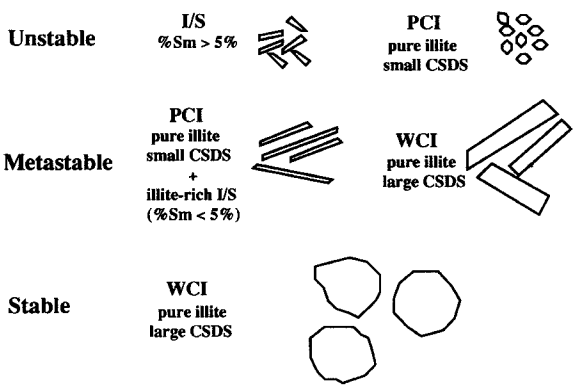

Figure 14. Sketch of the different states of I/S and illite particles in shales establishing the relations between XRD data (I/S, PCI and WCI) and morphology (small, large, very large, lath-shaped, isometric).

The normalized diameter and the log-normal distribution for all particles, as well as for isometric and lath particles considered separately, are presented on Figure 13. The α and β^2 values determined for these three types of distribution are very close: $\alpha = -0.134$ and $\beta^2 = 0.265$; $\alpha = -0.135$ and $\beta^2 = 0.263$; $\alpha = -0.134$ and $\beta^2 = 0.258$, for all particles, lath particles and isometric particles, respectively. Both lath and isometric particle populations are fitted by similar log-normal curves. The interpretation of these curves in terms of growth process is at least ambiguous, because isometric particles become predominant while lath-shaped ones progressively dissolve. The distribution of grain sizes according to a log-normal law implicates a reaction of second order (Chai 1974, Baronnet 1982). Whitney and Velde (1993) have shown that particle growth may result from three different processes: epitaxial nucleation and growth, coalescence, infilling and syntaxial growth. Because these mechanisms and their reaction order are poorly known, their characterization by indirect methods is questionable.

It is established that the stable phase in sandstones which experienced burial diagenesis is represented by the large hexagonal WCI particles (Lanson and Champion 1991). This is also the case in shales, even if the morphologies are not strictly similar: 1) laths are less elongated; 2) there is no hexagonal shapes but isometric particles often present two to three sharp faces. The WCI particles grow slowly with increasing depth through a series of intermediate steps during which composition, size and shape of particles change. These steps can be identified even if it is difficult to establish quantitative mass-balance of mineral reactions in diagenetic environment (Awwiller 1993). Chemical components consumed by growing WCI particles probably originate from two sources. The first one, which is the most active, is the dissolution of both small lath-shaped (I/S) and isometric particles (PCI), which are highly un-

https://doi.org/10.1346/CCMN.1995.0430103 Published online by Cambridge University Press

stable because of composition (expandable layers in I/S) and high surface energy (PCI). The second one, which is activated in the deepest part of the diagenetic series, is the dissolution of large PCI (illite-rich I/S + illite) and very large WCI (illite) lath-shaped particles. Both PCI and WCI purely illitic lath-shaped particles must be considered as the metastable state of illite. The stable state is reached with the growing WCI isometric particles. Figure 14 summarizes the different shapes and states of I/S, PCI and WCI particles.

CONCLUSION

The transformation of I/S and illitic particles basing the data here could be explained by two reactions with different kinetics:

1) The fastest reaction involves the precipitation of illite layers on I/S nuclei leading to large and very large lath-shaped particles of PCI and WCI composition, respectively. These particles represent a metastable state of the illite phase. Such nucleation mechanism has been suggested in natural and experimental systems (Pollastro 1985, Whitney and Velde 1993).
2) The slowest reaction involves the growth of isometric particles (WCI) which are pure high-charge illite. The formation of the largest particles may result from a complex mechanism involving epitaxial nucleation or syntaxial growth of aggregates (Whitney and Velde 1993). These particles represent the stable state of illite, the composition and the crystal shape of which result from the rule of minimization of the free energy of formation. The unstable state corresponds to I/S and small isometric illite particles (PCI), which are far from equilibrium because of variable chemical composition and high surface energy, respectively.

The two reactions are controlled by the formation of illite layers on both lath-shaped and isometric particles. The question is, what is the composition of these additional illite layers? It was shown in other diagenetic systems that the chemical composition of illite is strictly fixed: high-charge Fe-Mg-rich illite (Meunier and Velde 1989, Lanson and Champion 1991, Środoń *et al* 1992). This means that fluids were saturated with respect to this single illite composition. Then, the unsolved questions are: how I/S particles can grow if the fluids are saturated with respect to illite? Does the smectite layer grow simultaneously with the illite ones?

ACKNOWLEDGMENTS

A. Varajão acknowledges the CNPq (Conselho Nacional de Desenvolvimento Científico e Tecnológico) for providing the financial support and the PETROBRAS (Petroleo Brasileiro S.A.) for providing the samples. The authors are greatly indebted to B. Lanson (Elf Aquitaine Production), B. Velde (Ecole Normale Supérieure, Paris), D. Beaufort (LPAH, University of Poitiers) and A. Bouchet (E.R.M. company) for critical reviews and valuable suggestions. The authors are grateful to the two reviewers, R. Pollastro and J. Środoń, for their constructive criticisms of the manuscript.

REFERENCES

Awwiller, D. N. 1993. Illite/smectite formation and potassium mass transfer during burial diagenesis of mudrocks: A study from the Texas Gulf Coast Paleocen-Eocen. *Journal of Sedimentary Petrology* **63**: 501–512.

Baronnet, A. 1982. Ostwald ripening in solution. The case of calcite and mica. *Estudios Geologicos* **38**: 185–198.

Boles, J. R., and S. G. Franks. 1979. Clay diagenesis in Wilcox Sandstone of Southwest Texas: Implications of smectite diagenesis on Sandstone cementation. *Journal of Sedimentary Petrology* **49**: 55–70.

Burst, J. F. 1969. Diagenesis of Gulf Coast clayed sediments and its possible relation to petroleum migration. *Amer. Assoc. Petrol. Geol. Bull.* **53**: 73–93.

Chai, B. H. T. 1974. Mass transfer of calcite during hydrothermal recrystallization. In *Geochemical Transport and Kinetics*. A. W. Hoffmann, B. J. Giletti, H. S. Yoder Jr., and R. A. Yund, eds. 205–218. Carnegie Institute, Washington, D.C.

Champion, D. 1989. Etude des mécanismes de transformation des interstratifiés illite-smectite au cours de la diagenèse: Ph.D. thesis. Université de Paris-Sud, Centre D'Orsay, 204 pp.

Eberl, D. D., and J. Środoń. 1988. Ostwald ripening and interparticle-diffraction effects for illite crystals. *Amer. Miner.* **73**: 1335–1345.

Eberl, D. D., J. Środoń, M. Kralik, B. E. Taylor, and Z. E. Peterman. 1990. Ostwald ripening of clays and metamorphic minerals. *Science* **248**: 474–477.

Fernandes, G. J. F., Z. V. Matos, A. M. F. Figueiredo, W. L. Fisher, and L. F. Brown Jr. 1981. Basin analysis of the rift phase and oil and gas play analysis, Sergipe-Alagoas Basin, Brasil: PETROBRAS/DEPEX. (internal report).

Freed, R. L., and D. R. Peacor. 1989. Variability in temperature of the smectite/illite reaction in Gulf Coast sediments. *Clay Miner.* **1**: 171–180.

Glassmann, J. R., S. Larter, N. Brieds, and P. D. Lundegard. 1989. Shale diagenesis in the Bergen High Area, North Sea. *Clays & Clay Miner.* **37**: 97–112.

Hay, R. L. 1970. Silicate reactions in three lithofacies of a semi-arid basin, Olduvai Gorge, Tanzania. Mineralogical Society of America Special Paper 3, 237–255.

Hay, R. L., and R. J. Moiola. 1963. Authigenic silicate minerals in Searles Lake, California. *Sedimentology* **2**: 312–332.

Hoffman, J., and J. Hower. 1979. Clay mineral assemblages as low grade metamorphic geothermometers: Application to the thrust faulted disturbed belt of Montana, USA. *Soc. Econ. Paleontol. Miner. Spec. Publ.* **26**: 55–79.

Hower, J., E. V. Eslinger, M. E. Hower, and E. A. Perry Jr. 1976. Mechanism of burial metamorphism of argilaceous sediments: Mineralogical and chemical evidence. *Geol. Soc. Amer. Bull.* **87**: 725–737.

Inoue, A. 1986. Morphological change in a continuous smectite to illite conversion series by scanning and transmission electron microscopies. *Journal of College of Arts and Sciences,* Chiba University, **B-19,** 23–33.

Inoue, A., N. Kohyama, R. Kitagawa, and T. Watanabe. 1987. Chemical and morphological evidence for the conversion of smectite to illite. *Clays & Clay Miner.* **35**: 111–120.

Inoue, A., B. Velde, A. Meunier, and G. Touchard. 1988.

Mechanism of illite formation during smectite to illite conversion in a hydrothermal system. *Amer. Miner.* **73**: 1325–1334.

Jackson, M. L. 1974. *Soil Chemical Analysis—Advanced Course,* 2nd ed. Madison, Wisconsin: Published by the author, 895 pp.

Keller, W. D., R. C. Reynolds, and A. Inoue. 1986. Morphology of clay minerals in the conversion series by scanning electron microscopy. *Clays & Clay Miner.* **34**: 187–197.

Lanson, B. 1990. Mise en évidence des mécanismes de transformation des interstratifiés illite/smectite au cours de la diagenèse: Ph.D. thesis. Université de Paris-Sud, Centre D'Orsay, France, 366 pp.

Lanson, B., and G. Besson. 1992. Characterization of the end of smectite-to-illite transformation: Decomposition of X-ray patterns. *Clays & Clay Miner.* **40**: 40–52.

Lanson, B., and D. Champion. 1991. The I/S-to-illite reaction in the late stage diagenesis. *Amer. J. of Sci.* **291**: 473–506.

Lanson, B., and B. Velde. 1992. Decomposition of X-ray diffraction patterns: A convenient way to describe complex I/S diagenetic evolution. *Clays & Clay Miner.* **40**: 629–643.

Meunier, A., and B. Velde. 1989. Solid solutions in illite/smectite mixed layer minerals and illite. *Amer. Miner.* **74**: 1106–1112.

Nadeau, P. H. 1985. The physical dimension of fundamental clay particles. *Clays & Clay Miner.* **20**: 499–514.

Nadeau, P. H., and R. C. Reynolds. 1981. Burial contact metamorphism in the Mancos Shale. *Clays & Clay Miner.* **29**: 249–259.

Perry, E., and J. Hower. 1970. Burial diagenesis in Gulf Coast pelitic sediments. *Clays & Clay Miner.* **18**: 165–177.

Pollastro, R. M. 1985. Mineralogical and morphological evidence for the formation of illite at the expense of illite/smectite. *Clays & Clay Miner.* **33**: 265–274.

Ponte, F. C., and H. E. Asmus. 1976. The Brazilian marginal basins: Current state of knowledge. *Acad. Bras. Cienc.,* São Paulo, Brasil, **48**: 215–240.

Remy, R. R., and R. Ferrell. 1989. Distribution and origin of analcime in marginal lacustrine mudstone of the Green River Formation, South-Central Uinta Basin, Utah. *Clays & Clay Miner.* **37**: 419–432.

Reynolds, R. C. 1985. NEWMOD: A computer program for the calculation of one-dimensional patterns of mixed-layered clays. R. C. Reynolds, 8 Brook Rd., Hanover, New Hampshire 03755.

Sato, T., T. Watanabe, and R. Otsuka. 1992. Effects of layer charge, charge location, and energy change on expansion properties of dioctahedral smectites. *Clays & Clay Miner.* **40**: 103–113.

Środoń, J., F. Elsass, W. J. McHardy, and D. J. Morgan. 1992. Chemistry of illite-smectite inferred from TEM measurements of fundamental particles. *Clay Miner.* **27**: 137–158.

Touchard, G., B. Velde, L. Cailleu, H. Badri, and J. Borzeix. 1993. Form analysis software by image processing. Applications to clay particles and soil structure. *Proceedings of 6ECS,* Prague, **12**: 263–268.

Velde, B., T. Suzuki, and E. Nicot. 1986. Pressure-temperature-composition of illite/smectite mixed-layer minerals. Niger delta mudstones and other examples. *Clays & Clay Miner.* **34**: 435–441.

Velde, B., and G. Vasseur. 1992. Estimation of the diagenetic smectite to illite transformation in time-temperature space. *Amer. Miner.* **77**: 967–976.

Whitney, G., and B. Velde. 1993. Changes in particle morphology during illitization: An experimental study. *Clays & Clay Miner.* **41**: 209–218.

(Received 21 February 1994; accepted 29 June 1994; Ms. 2472)